ACCURACY OF COMPUTED TOMOGRAPHY IN DETERMINING LESION SIZE IN CANINE OSTEOSARCOMA OF THE APPENDICULAR SKELETON

Thesis

Presented in Partial Fulfillment for the Requirements for the Degree of Master of Science in the Graduate School of The Ohio State University

By

Ketaki S. Karnik, DVM

Graduate Program in Comparative and Veterinary Medicine

The Ohio State University
2011

Thesis Committee:

Dr. Eric M. Green, Advisor

Dr. Steven E. Weisbrode

Dr. Cheryl A. London

ABSTRACT

Multidetector contrast enhanced computed tomography with acquisition of 0.625 mm thick axial transverse images was used to measure the extent of appendicular osteosarcoma (OSA) in 10 dogs. The measured length of tumor based on CT was compared to the true length of tumor using histopathology. There was good correlation of the true length of OSA compared to the length of intramedullary/endosteal abnormalities on CT with a mean overestimation of 1.8% (SD = 15%). There was poor correlation of the true length of OSA compared to the length of periosteal proliferation on CT with a mean overestimation of 9.7% (SD = 30.3%). There was poor correlation of the true length of OSA compared to the length of abnormal contrast enhancement by 9.6% (SD = 34.8%). The measured extent of intramedullary/endosteal abnormalities using sub-millimeter thick axial transverse acquisition of images with multidetector CT should be of value in assessing patient candidacy and surgical margins for limb spare surgery. It may also be useful for evaluating response to therapy in dogs that receive chemotherapy or radiation therapy when surgery is not performed.

ACKNOWLEDGMENTS

To my loving parents and brother for their support.

To Sarah, who was my inspiration and motivation for this study, and my career.

To my mentors, Drs. Eric Green and Valerie Samii, for always being supportive and teaching me the importance of staying positive and enthusiastic in life and at work.

To my mentors Drs. Zekas, Drost, and Murakami, for exposing me to the joys of diagnostic imaging and teaching me to stay open-minded and reasonable.

To Drs. Steven Weisbrode and Cheryl London for their patience, advice, and always making time for me.

To Dr. Rita Echandi for her advice and insight.

To all of the caring pet owners and their dogs for their participation which made this study possible.

To The American College of Veterinary Radiology and The Ohio State University Intramural Canine Grant Fund for funding this study.

VITA

2001	Bachelor of Science, Microbiology and Molecular Genetics University of California, Los Angeles
2005	Doctor of Veterinary Medicine University of California, Davis
2005-2006	Internship – Small Animal Medicine and Surgery VCA West Los Angeles Animal Hospital
2008-2011	Resident in Veterinary Diagnostic Imaging Veterinary Medical Center The Ohio State University
2008-2011	Master of Science in Veterinary Clinical Sciences College of Veterinary Medicine The Ohio State University

AWARDS

2009 American College of Veterinary Radiology Resident Research Award
"Accuracy of Computed Tomography in Determining Lesion Size in Canine Osteosarcoma of the Appendicular Skeleton"

PUBLICATIONS

Karnik KS, Reichle JK, Fischetti AJ, Goggin JM. Computed Tomographic Findings of Fungal Rhinitis and Sinusitis in Cats. *Veterinary Radiology and Ultrasound*, 2009;50: 65-68.

Grant IA, **Karnik KS**, Jandrey KE. Toxicities and Salvage Therapy Following Overdose of Vinblastine in a Cat. *Journal of Small Animal Practice*, 2010;51:127-131.

FIELDS OF STUDY

Major Field: Comparative and Veterinary Medicine

Specific Field: Veterinary Diagnostic Imaging

TABLE OF CONTENTS

Page

LIST OF FIGURES

(window width = 350, window level = 50).

Figure 4……

There is good correlation of tumor length based on histopathology compared to the length of intramedullary/endosteal abnormalities based on CT. There is good correlation of the data to the regression line ($r^2 = 0.85$). The slope of the regression line is 0.98 with a y-intercept of 1.1, indicating a near direct linear relationship. P-value slope = 0.0001.

Figure 5…….

There is poor correlation of tumor length based on histopathology compared to the length of periosteal proliferation based on CT. Slope = 0.67, y-intercept = 49.4, $r^2 = 0.27$, p-value slope = 0.1225.

Figure 6……..

There is poor correlation of tumor length based on histopathology compared to the length of abnormal contrast enhancement based on CT. Slope = 0.59, y-intercept = 50.1, $r^2 = 0.42$, p-value slope = 0.0419.

Figure 7……..

Distribution of percent overestimation and underestimation of the predictive value of intramedullary/endosteal abnormalities on CT compared to the true length of neoplasia based on histopathology.

Figure 8……

(A) Transverse CT image of OSA of the tibia. Note the lack of periosteal proliferation.

(B) Histopathologic slide at the same level. There is evidence of periosteal hyperplasia (black arrow) transitioning from a more normal periosteum (white arrow).

CHAPTER 1

INTRODUCTION

Osteosarcoma (OSA) is the most common primary bone tumor in dogs and is associated with poor prognosis and rapid progression of disease.[1-4] The majority of primary OSA lesions affect the appendicular skeleton. In a study of 183 dogs with OSA, 77% of the lesions were located at appendicular sites.[2] In a separate study of 38 dogs, 94.7% had appendicular OSA.[1] Treatment for OSA of the limb includes chemotherapy, radiation therapy, limb amputation, and limb spare surgery. These treatments may be performed in combination or individually. Although less than 15% of dogs with OSA have radiographic evidence of pulmonary or osseous metastasis at presentation, approximately 90% will die from metastasis within one year when amputation is the only treatment.[5] Thus treatment of the primary lesion by amputation or resection of diseased bone alone is rarely curative.

While limb amputation is typically employed to remove the primary tumor, it may not be an option due to severe orthopedic disease, neurologic disease, large body size, or owner preference.[6] For these dogs, limb spare techniques involving replacement of diseased bone with non-diseased bone or an endoprosthesis have been developed. Limb

spare procedures in the dog have been described for the distal radius[7-11], proximal humerus[12], distal tibia[13], and proximal femur[14].

With limb spare techniques, accurate determination of the surgical excision margin is critical as there is a higher risk of implant failure if greater than 50% of the bone is affected and inadequate excision carries a higher risk for local recurrence.[15-17] In a study of 220 dogs that underwent limb spare surgery for treatment of OSA, local recurrence occurred in 25% of dogs after one year.[18] In a separate study of limb spare surgeries involving the humerus, local recurrence occurred in 24% of dogs.[12] The incidence of metastasis may also be influenced by surgical margins. In a study of dogs receiving adjuvant chemotherapy for humeral OSA, those with incomplete surgical margins were 7.7 times more likely to develop metastasis than those with complete resection.[12]

To our knowledge, an objective method to accurately assess the response of appendicular OSA to treatment has not been described. Previous attempts to monitor the response of OSA to chemotherapeutic agents have involved *in vitro* testing with isolated canine cancer cell lines or mean survival comparisons.[1, 19] *In vitro* techniques and xenograft models are used in human medicine to monitor the response of sarcomas, including OSA, to various treatments.[20, 21] Response of appendicular OSA to radiotherapy in dogs has been evaluated by monitoring changes in limb function or subjectively assessing pain relief.[22-24] Pain relief following radiotherapy has been measured using force plate analysis, however actual regression or progression of OSA was not proven.[25]

Recent studies have investigated the accuracy of measuring the length of appendicular OSA lesions using a variety of diagnostic imaging techniques. Bone scintigraphy with Technetium-99m labeled methylene diphosphonate (^{99m}Tc-MDP) and craniocaudal and lateromedial projection radiographs demonstrated a mean overestimation of the length of OSA compared to the true length of OSA based on histopathology.[26, 27] Magnetic resonance imaging (MRI) demonstrated a mean overestimation of OSA length by 3 +/- 13% in one study and an overestimation ranging from 0.4 to 4.4 cm in another.[6, 26] Non-contrast enhanced computed tomography (CT) has also been used to objectively measure the length of appendicular OSA. There was a mean overestimation of OSA by CT of 27 +/- 36% in one study in which 1.5 mm thick sagittal images of the entire length of the affected bone were acquired.[26] There was overestimation of tumor margins in 8/9 dogs ranging from 0.1 to 4.6 cm in another study in which 5 mm thick transverse images were acquired through the length of the affected bone.[6] These previous CT based studies did not employ multidetector technology which enables acquisition of sub-millimeter collimated transverse images allowing for more precise measurements to be made. Also, since these previous studies were performed post amputation, intravenous contrast medium was not administered.

Because accurate determination of the extent of appendicular OSA is of importance for surgical margins and patient candidacy for limb spare procedures and also in serial monitoring of response to chemotherapy or radiotherapy when amputation is not performed, developing more accurate imaging methods is critical. Therefore, the purpose of this preliminary study was to evaluate the accuracy of pre- and post contrast

multidetector CT detection of appendicular OSA in dogs compared to the "gold standard" of histopathology. Our null hypothesis was that multidetector contrast enhanced CT would not correlate with histopathologic measurements in assessing the extent of appendicular OSA.

CHAPTER 2

MATERIALS AND METHODS

This was a prospective study of 10 client owned dogs that presented to The Ohio State University Veterinary Medical Center. The patients ranged from 4-12 years of age. The breeds represented were 8 Greyhounds, 1 Saint Bernard, and 1 Labrador Retriever. The following sites of OSA were represented among the dogs: proximal humerus (4), distal femur (2), proximal tibia (1), distal tibia (1), distal radius (1), and mid-distal ulna (1). Dogs with radiographic findings of aggressive bone disease of the appendicular skeleton compatible with primary bone neoplasm were screened for inclusion. A presumptive diagnosis of OSA was made based on the combination of clinical findings, radiographs, and cytologic evidence of mesenchymal neoplasia.[28, 29] Cytologic evidence was obtained with ultrasound guided fine needle aspiration of diseased bone (Sequoia 512, Acuson, Malvern, PA; MyLab 70, Biosound Esaote, Indianaopolis, IN). Patients with radiographic evidence of a pathologic fracture or those that had received prior chemotherapy or radiation therapy were excluded from the study. The presence of a fracture/s would have made it difficult to accurately measure sections for histopathologic measurements post amputation. In addition, chemotherapy and radiation cause cell death

and there was the concern that contrast enhancement would be altered in patients that had received these treatments. All patients were scheduled for limb amputation for the treatment of primary bone neoplasia. A diagnosis of osteosarcoma was histopathologically confirmed via biopsy post amputation in all patients. Client consent was obtained prior to participation in the study.

Patients were anesthetized using a patient specific anesthetic protocol. An intravenous catheter was placed for administration of anesthetic and CT contrast agents in a non-affected limb. Patients were positioned either in dorsal or ventral recumbency, depending on patient conformation and ease of positioning. The affected and contralateral bones were symmetrically positioned within the CT gantry, parallel to the table. A series of 0.625 mm thick axial transverse contiguous images were acquired perpendicular to the long axis of the affected and contralateral bone (Lightspeed 3.X, GE Healthcare, Waukesha, WI). The scan included at least 1 cm proximal and distal to the articular margin of the affected bone. Image acquisition parameters were set at kVp = 100 and mA = 130. The field of view was large enough to include both the affected and contralateral bones for comparison purposes. Images were acquired using a bone algorithm (window width = 2500-3500, window level = 250-350) and reconstructed into a standard algorithm (window width = 350-400, window level = 40-50) (Figure 1). Iohexol 240 mg I/ml (Omnipaque, GE Healthcare, Princeton, NJ) at a dose of 2 ml/kg was hand injected intravenously and the initial acquisition was immediately repeated using a standard algorithm and identical limb positioning. The total scan time (pre- and post contrast) required for image acquisition was approximately 16 to 20 minutes. The

CT scan was immediately followed by limb amputation.

The CT images were evaluated as a group among two ACVR Diplomates and a radiology resident (EMG, VFS, KSK). Window width and window level were adjusted as needed. The following 3 CT lesions were measured for each OSA affected bone: the length of intramedullary/endosteal abnormalities, the length of periosteal proliferation, and the length of abnormal contrast enhancement. The contralateral bone was used as a control for comparison. The criteria for intramedullary/endosteal abnormalities included any changes in intramedullary attenuation (hypo- or hyperattenuation) or irregularity adjacent to the internal cortical margin that was not seen in the contralateral bone at the same level (Figure 2). The criterion for periosteal proliferation was the presence of any periosteal new bone that was not seen along the contralateral bone in the identical region. Abnormal contrast enhancement was confirmed by measuring the Hounsfield Units (HU) using regions of interest within the medullary cavity of the affected versus contralateral bone at the same level (Figure 3). Any increase in HU relative to the contralateral bone was considered abnormal. The length of the lesion was measured from the articular surface closest to the tumor to the furthest extent of disease. Transverse images were used to make the measurements using digital software (eFilm, Merge Healthcare, Milwaukee, WI). The soft tissues surrounding the bones were not evaluated.

Histopathology served as the gold standard for measuring the true extent of neoplasia and was also used to confirm the diagnosis of OSA. Following amputation, 1 cm thick transverse sections were made through the affected bone using a band saw. Each section was then individually re-measured using electronic calipers to within 0.01

mm. The bone loss caused by the band saw was taken into consideration by adding the width of the blade between individual sections. The sections were placed in 10% buffered formalin for at least 72 hours followed by a decalcification solution of 50% formic acid for 2-5 weeks. The sections were then cut transversely with a blade to approximately 5.0 mm and individually re-measured to within 0.01 mm. These sections were processed and embedded in paraffin. Transverse 5 μm thick slices were made at 500 μm increments through the processed sections using a microtome (Leitz 1512, Wetzlar, Germany) and mounted on slides. The slides were routinely stained with hematoxylin and eosin.

The slides were evaluated by a board certified veterinary pathologist (SEW) for evidence of periosteal, intramedullary, and endosteal neoplasia. The extent of neoplasia was determined to be the furthest extension of neoplastic cells regardless of periosteal, intramedullary, or endosteal involvement. The extent of neoplasia was determined to be at the slice between the presence and absence of neoplastic cells to within 500 μm. In the event that the transition between neoplastic and non-neoplastic cells occurred at the junction of a band saw or blade cut, the extent of neoplasia was considered to be between the two sections, 500 μm distal or proximal to the last section containing neoplastic cells.

Linear regression analysis was used to create a statistical model based on the CT and histopathology lesion lengths obtained for each patient. The length of each CT lesion (intramedullary/endosteal abnormalities, periosteal proliferation, abnormal contrast

enhancement) was then correlated to the true length of neoplasia using the predictive model. Statistical tests were performed using statistical software (SAS, Cary, NC; Excel, Microsoft, Redmond, WA).

CHAPTER 3

RESULTS

Intramedullary neoplasia extended further than endosteal and periosteal neoplasia based on histopathologic analysis in all patients. Since each of the following 3 CT characteristics were compared to the furthest extent of tumor, they were each compared to the length of intramedullary neoplasia measured via histopathology.

CT intramedullary/endosteal abnormalities

All 10 dogs had abnormalities within the intramedullary cavity of the affected bone on CT. There was good prediction of the true extent of neoplasia on histopathology based on the length of intramedullary/endosteal abnormalities measured on CT (slope = 0.98, y-intercept = 1.1, $r^2 = 0.85$, p-value slope = 0.0001) (Figure 4). The relatively high r^2 value indicates that the data fits the statistical model well. There was a mean overestimation of tumor length of 1.8% (SD = 15%). CT overestimated the length of neoplasia based on intramedullary/endosteal abnormalities in 7/10 dogs ranging from 0.08% to 27.1%. CT underestimated the length of neoplasia in 3/10 dogs ranging from 3.3% to 29.5%.

CT periosteal proliferation

All 10 dogs had CT evidence of periosteal proliferation of the affected bone. There was poor prediction of the true extent of neoplasia on histopathology based on the length of periosteal proliferation measured on CT (slope = 0.67, y-intercept = 49.4, r^2 = 0.27, p-value slope = 0.1225) (Figure 5). There was a mean overestimation of tumor length of 9.7% (SD = 30.3%).

CT overestimated the length of neoplasia based on periosteal proliferation in 7/10 dogs ranging from 0.03% to 60.9%. Of the 7 dogs in which the intramedullary/endosteal abnormalities on CT overestimated tumor length, 6 of the same dogs were also overestimated using periosteal proliferation. In the other dog, the extent of periosteal proliferation overestimated the length of tumor by 26.3% whereas it was underestimated by 3.3% using intramedullary/endosteal abnormalities.

Periosteal proliferation on CT underestimated tumor length in 3/10 dogs ranging from 3.7% to 46.4%. Of the 3 dogs in which intramedullary/endosteal abnormalities underestimated the extent of tumor, 2 of the same dogs were also underestimated using periosteal proliferation. In the other dog, the extent of periosteal proliferation underestimated the length of tumor by 23.9% whereas it was overestimated by 0.08% using intramedullary/endosteal changes.

CT abnormal contrast enhancement

All 10 dogs had evidence of abnormal contrast enhancement within the medullary cavity of the affected bone. There was poor prediction of the true extent of neoplasia on

histopathology based on the length of abnormal contrast enhancement measured on CT (slope = 0.59, y-intercept = 50.1, r^2 = 0.42, p-value slope = 0.0419) (Figure 6). There was a mean overestimation of tumor length of 9.6% (SD = 34.8%).

CT overestimated the length of neoplasia based on abnormal contrast enhancement in 7/10 dogs ranging from 0.47% to 62.8%. These were also the same 7 dogs in which OSA was overestimated using the extent of periosteal proliferation. Of the 7 dogs in which the intramedullary/endosteal abnormalities on CT overestimated tumor length, 6 of the same dogs were also overestimated using abnormal contrast enhancement. In the other dog, the extent of abnormal contrast enhancement overestimated the length of OSA by 35.8% whereas it was underestimated by 3.3% using intramedullary/endosteal abnormalities.

CT underestimated the length of neoplasia based on abnormal contrast enhancement in 3/10 dogs ranging from 22.5% to 47.4%. These were the same 3 dogs in which OSA was underestimated based on the extent of periosteal proliferation on CT. Of the 3 dogs in which intramedullary/endosteal abnormalities underestimated the extent of tumor, 2 of the same dogs were also underestimated using abnormal contrast enhancement. In the other dog, the extent of abnormal contrast enhancement underestimated the length of tumor by 47.4% whereas it was overestimated by 0.08% using intramedullary/endosteal abnormalities.

CHAPTER 4

DISCUSSION

Intramedullary/endosteal neoplasia was the furthest extending tumor location in all patients based on histopathology. Consequently, each of the 3 CT characteristics (intramedullary/endosteal abnormalities, periosteal proliferation, abnormal contrast enhancement) were compared to intramedullary/endosteal neoplasia on histopathology since it represented the furthest extent/maximum length of OSA.

The CT characteristic that was the best predictor of the length of OSA was the length of intramedullary/endosteal abnormalities. Despite this, it is important to consider that tumor length was underestimated in 3 patients, which would have lead to incomplete resection of tumor margins (Figure 7). In one Greyhound that had OSA of the proximal humerus, the extent of tumor was underestimated by 29.5% or 34.8 mm. If the mean overestimation and one standard of deviation of 1.8% (SD = 15.0%) were included in the surgical resection, tumor would have been completely resected in all but this one patient.

The extent of periosteal proliferation seen on CT was a poor predictor of tumor length. There was a mean overestimation of tumor length of 9.7% (SD = 30.3%). Interestingly, in some patients, evidence of periosteal hyperplasia seen on histopathology

was not seen on CT (Figure 8). This may have occurred because the thickness of the histological sections was 0.500 mm, which was thinner than the CT image thickness of 0.625 mm. Due to volume averaging within the CT image voxel, there was the chance that small lesions were not resolved. These discrepancies may have contributed to the poor estimation of tumor length based on periosteal proliferation on CT.

The extent of abnormal contrast enhancement was a poor predictor of tumor length. In fact, the scatter plot of intramedullary tumor to abnormal contrast enhancement on CT demonstrated more of a U-shaped curve rather than a line. Quadratic linear regression analysis would have been better fit than linear analysis, however it was impractical to use since we were evaluating the direct relationship of true tumor length to CT. Using linear regression analysis, there was a mean overestimation of tumor length of 9.6% (SD = 34.8%) using abnormal contrast enhancement on CT as a predictor.

Tumor necrosis may have contributed to the underestimation of tumor length based on abnormal contrast enhancement on CT. The lack of vascularity in necrotic regions could have lead to a lack of contrast enhancement despite the presence of neoplastic cells. In fact, there were gaps of abnormal contrast enhancement within the intramedullary cavity of some patients. Abnormal contrast enhancement could be followed for several millimeters, followed by non-contrast enhancing tissue, and then transition back into abnormal contrast enhancing tissue. These gaps of non-contrast enhancing tissue may have represented regions of tumor necrosis. Tissue necrosis was not evaluated on histopathology.

Another explanation for the gaps of abnormal contrast enhancement could be skip metastasis. Skip metastasis has been reported in the human literature. This refers to a simultaneous smaller focus of OSA separate from the primary lesion within the same bone or on the opposing side of the adjacent joint.[30] In this study, skip metastasis was not evaluated as only the first transition from neoplastic to non-neoplastic cells was considered to be the extent of tumor. The entire bone was not histologically evaluated.

In addition, it was difficult to evaluate contrast enhancement in regions of sclerotic or cancellous bone. Subtle changes in contrast enhancement did not cause a significant change in HU in these regions due to the inherently high HU values in bone. This may have also contributed to the poor predictive value of abnormal contrast enhancement.

Based on our data, multidetector CT with acquisition of sub-millimeter thick images appeared to be a better predictor of the extent of neoplasia compared with non-multidetector CT studies performed previously. This was likely due to the ability to acquire axial images as thin as 0.625 mm which allowed for more precise measurements to be made compared to helical acquisition of thicker images in previous studies. In addition, although sagittal and dorsal reformatted images were available, measurements were based off of continuous transverse images. This enabled evaluation of the entire cross section of bone at once for any abnormalities.

One of the limitations in this study was acquisition time. The acquisition of axial sub-millimeter thick images through the entire length of bone took an average of 8 to 10 minutes. This was repeated following contrast medium administration for a total of 16 to

20 minutes. The long acquisition time could have lead to dissipation of contrast medium prior to complete imaging. However, since contrast enhancement was not a good predictor of tumor length, we believe that contrast medium administration would be unnecessary in identifying the leading edge of tumor, reducing scan and anesthesia time. It may still be of value in monitoring response of chemotherapy and radiation therapy when surgery is not performed.

Another limitation of this study was accuracy in measurement of the histological sections. Each section was individually processed and placed in paraffin. The thickness of the paraffin prior to sectioning could not be quantified and had the potential to result in mild over or underestimation of the histopathological measurements. In addition, the tissue block may not have been level within the paraffin block, leading to asymmetric tissue slicing.

Tissue processing may have also lead to dehydration and subsequent shrinkage of the specimens leading to a change in tissue thickness. In a recent study using a porcine model, there was no change in bone volume or diameter measured by MRI following formalin fixation.[31] To our knowledge, the effects of decalcification on bone have not been studied.

In addition, if the transition of neoplastic to non-neoplastic cells occurred at the junction of a band saw or blade cut, the tumor was assumed to be 500 μm distal or proximal to the last neoplastic slice. This may have lead to mild over or underestimation of the true extent of neoplasia. Also, although the amount of bone loss between sections was assumed to be the width of the band saw blade, the true amount of bone loss was

likely greater due to the oscillation of the blade while sectioning.

It is acknowledged that some dogs with appendicular osteosarcoma have a significant soft tissue component that would preclude limb spare surgery.[18] This was not addressed in this study, but future studies should be performed to evaluate the significance of such lesions.

The majority of patients in our study were Greyhounds (80%). Greyhounds have a variety of hematologic and pathologic processes that differ from other breeds of dogs[32-36]. The predominance of Greyhounds in our study could have resulted in different data compared to a study in which Greyhounds did not predominate. Breed and biologic differences should be considered during evaluation of OSA.

Based on this preliminary study, the length of intramedullary/endosteal abnormalities using transverse sub-millimeter thick axial acquisition of images with multidetector CT correlated well with the length of appendicular OSA. This should be of value in assessing patient candidacy and surgical margins in limb spare surgery. It may also be useful for evaluating response to therapy in dogs that receive chemotherapy or radiation therapy when surgery is not performed. Further studies should be performed in the future, using more patients, to corroborate the significance of this study.

BIBLIOGRAPHY

1. Mauldin GN, Matus RE, Withrow SJ, Patnaik AK. Canine osteosarcoma treatment by amputation versus amputation and adjuvant chemotherapy using doxorubicin and cisplatin, *J Vet Intern Med* 1988;2:177-180.

2. Liu SK, Dorfman HD, Hurvitz AI, Patnaik AK. Primary and secondary bone tumours in the dog, *J Small Anim Pract* 1977;18:313-326.

3. Probst CW AN. Malignant neoplasia of the canine appendicular skeleton, *Comp Cont Educ Pract* 1982:260-270.

4. Brodey RS, Sauer RM, Medway W. Canine bone neoplasms, *J Am Vet Med Assoc* 1963;143:471-495.

5. Dernell WS, Ehrahrrt NP, Straw RC, Vail DM. In: Withrow SJ, Vail DM, editors. Small Animal Clinical Oncology. Tumors of the skeletal system. Missouri: Saunders; 2007. 540-582. In: Anonymous .

6. Davis GJ, Kapatkin AS, Craig LE, Heins GS, Wortman JA. Comparison of radiography, computed tomography, and magnetic resonance imaging for evaluation of appendicular osteosarcoma in dogs, *J Am Vet Med Assoc* 2002;220:1171-1176.

7. Liptak JM, Dernell WS, Ehrhart N, Lafferty MH, Monteith GJ, Withrow SJ. Cortical allograft and endoprosthesis for limb-sparing surgery in dogs with distal radial osteosarcoma: a prospective clinical comparison of two different limb-sparing techniques, *Vet Surg* 2006;35:518-533.

8. Liptak JM, Ehrhart N, Santoni BG, Wheeler DL. Cortical bone graft and endoprosthesis in the distal radius of dogs: a biomechanical comparison of two different limb-sparing techniques, *Vet Surg* 2006;35:150-160.

9. Seguin B, Walsh PJ, Mason DR, Wisner ER, Parmenter JL, Dernell WS. Use of an ipsilateral vascularized ulnar transposition autograft for limb-sparing surgery of the distal radius in dogs: an anatomic and clinical study, *Vet Surg* 2003;32:69-79.

10. Pooya HA, Seguin B, Mason DR, Walsh PJ, Taylor KT, Kass PH, Stover SM. Biomechanical comparison of cortical radial graft versus ulnar transposition graft limb-sparing techniques for the distal radial site in dogs, *Vet Surg* 2004;33:301-308.

11. Jehn CT, Lewis DD, Farese JP, Ferrell EA, Conley WG, Ehrhart N. Transverse ulnar bone transport osteogenesis: a new technique for limb salvage for the treatment of distal radial osteosarcoma in dogs, *Vet Surg* 2007;36:324-334.

12. Kuntz CA, Asselin TL, Dernell WS, Powers BE, Straw RC, Withrow SJ. Limb salvage surgery for osteosarcoma of the proximal humerus: outcome in 17 dogs, *Vet Surg* 1998;27:417-422.

13. Rovesti GL, Bacucci M, Schmidt K, Marcellin-Little DJ,. Limb sparing using a double bone-transport technique for treatment of a distal tibial osteosarcoma in a dog, *Vet Surg* 2002;31:70-77.

14. Liptak JM, Pluhar GE, Dernell WS, Withrow SJ. Limb-sparing surgery in a dog with osteosarcoma of the proximal femur, *Vet Surg* 2005;34:71-77.

15. Buracco P, Morello E, Martano M, Vasconi ME. Pasteurized tumoral autograft as a novel procedure for limb sparing in the dog: a clinical report, *Vet Surg* 2002;31:525-532.

16. Boston SE, Duerr F, Bacon N, LaRue S, Ehrhart EJ, Withrow S. Intraoperative radiation for limb sparing of the distal aspect of the radius without transcarpal plating in five dogs, *Vet Surg* 2007;36:314-323.

17. LaRue SM, Withrow SJ, Powers BE, Wrigley RH, Gillette EL, Schwarz PD, Straw RC, Richter SL. Limb-sparing treatment for osteosarcoma in dogs, *J Am Vet Med Assoc* 1989;195:1734-1744.

18. Straw RC WS. Limb-sparing surgery versus amputation for dogs with bone tumors, *Vet Clin North Am Small Anim Pract* 1996;26:135-143.

19. Kisseberth WC, Murahari S, London CA, Kulp SK, Chen C. Evaluation of the effects of histone deacetylase inhibitors on cells from canine cancer cell lines, *Am J Vet Res* 2008;69:938-945.

20. Garg V, Zhang W, Gidwani P, Kim M, Kolb EA. Preclinical analysis of tasidotin HCl in Ewing's sarcoma, rhabdomyosarcoma, synovial sarcoma, and osteosarcoma, *Clin Cancer Res* 2007;13:5446-5454.

21. Morton CL, Favours EG, Mercer KS, Boltz CR, Crumpton JC, Tucker C, Billups CA, Houghton. Evaluation of ABT-751 against childhood cancer models in vivo, *Invest New Drugs* 2007;25:285-295.

22. McEntee MC, Page RL, Novotney CA, Thrall DE. Palliative radiotherapy for canine appendicular osteosarcoma, *Vet Radiol Ultrasound* 1993;34:367-370.

23. Ramirez O, Dodge RK, Page RL, Price GS, Hauck ML, LaDue TA, Nutter F, Thrall DE. Palliative radiotherapy of appendicular osteosarcoma in 95 dogs, *Vet Radiol Ultrasound* 1999;40:517-522.

24. Fan TM, Charney SC, de Lorimier LP, Garrett LD, Griffon DJ, Gordon-Evans WJ, Wypij JM. Double-blind placebo-controlled trial of adjuvant pamidronate with palliative radiotherapy and intravenous doxorubicin for canine appendicular osteosarcoma bone pain, *J Vet Intern Med* 2009;23:152-160.

25. Weinstin JI, Payne S, Poulson JM, Azuma C. Use of force plate analysis to evaluate the efficacy of external beam radiation to alleviate osteosarcoma pain, *Vet Radiol Ultrasound* 2009;50:673-678.

26. Wallack ST, Wisner ER, Werner JA, Walsh PJ, Kent MS, Fairley RA, Hornof WJ. Accuracy of magnetic resonance imaging for estimating intramedullary osteosarcoma extent in pre-operative planning of canine limb-salvage procedures, *Vet Radiol Ultrasound* 2002;5:432-441.

27. Leibman NF, Kuntz CA, Steyn PF, Fettman MJ, Powers BE, Withrow SJ, Dernell WS. Accuracy of radiography, nuclear scintigraphy, and histopathology for determining the proximal extent of distal radius osteosarcoma in dogs, *Vet Surg* 2001;30:240-245.

28. Samii VF, Nyland TG, Werner LL, Baker TW. Ultrasound-guided fine needle aspiration biopsy of bone lesions: a preliminary report, *Vet Radiol Ultrasound* 1999;40:82-86.

29. Vignolli M, Ohlerth S, Rossi F, Pozzi L, Terragni R, Corlazzoli D, Kaser-Hotz B. Computed tomography-guided fine-needle aspiration and tissue-core biopsy of bone lesions in small animals, *Vet Radiol Ultrasound* 2004;45:125-130.

30. Enneking WF KA. Skip metastases in osteosarcoma, *Cancer* 1975;36:2192-2205.

31. Docquier P, Paul L, Cartiaux O, Lecouvet F, Dufrane D, Delloye C, Galant C. Formalin fixation could interfere with the clinical assessment of the tumor-free margin in tumor surgery: magnetic resonance imaging-based study, *Oncology* 2010;78:115-124.

32. Clemente M, Marin L, Iazbik MC, Couto CG. Serum concentrations of IgG, IgA, and IgM in retired racing Greyhound dogs, *Vet Clin Pathol* 2010;39:436-439.

33. Drost WT, Couto CG, Fischetti AJ, Mattoon JS, Iazbik C. Comparison of glomerular filtration rate between Greyhounds and non-Greyhound Dogs, *J Vet Intern Med* 2006;20:544-546.

34. Feeman WE, Couto CG, Gray TL. Serum creatinine concentrations in retired racing greyhounds, *Vet Clin Pathol* 2003;32:40-42.

35. Shiel RE, Brennan SF, O' Rourke LG, McCullough M, Mooney CT. Hematologic values in young pretraining healthy Greyhounds, *Vet Clin Pathol* 2007;36:274-277.

36. Vilar P, Couto CG, Westendorf N, Iazbik C, Charske J, Marin L. Thromboelastographic tracings in retired racing Greyhounds and in non-Greyhound dogs, *J Vet Intern Med* 2008;22:374-379.

APPENDIX

FIGURES

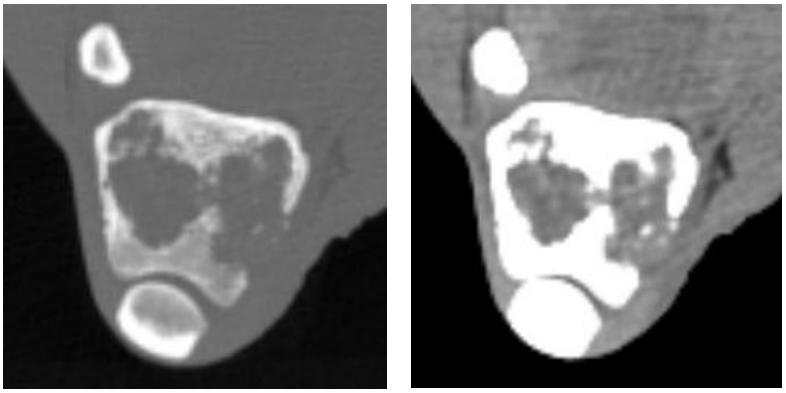

A B

Figure 1. (A) Transverse image of OSA of the distal femur in a bone algorithm (window width = 2500, window level = 250). There is multifocal medullary and cortical lysis. (B) Same image reconstructed into a standard algorithm (window width = 400, window level = 40).

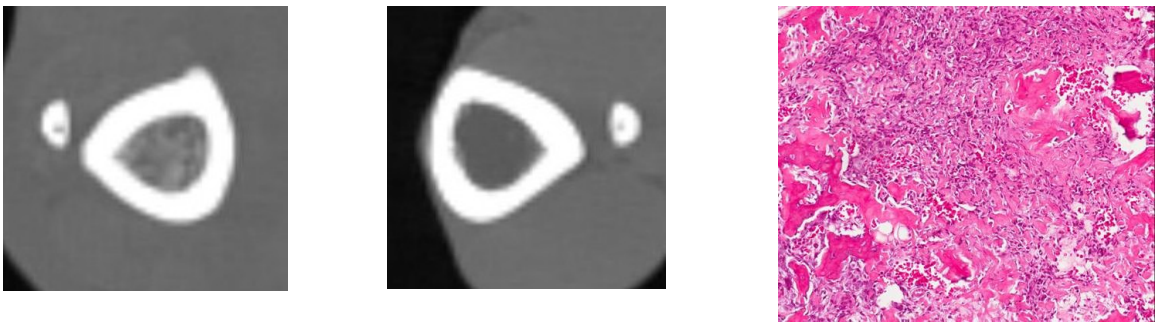

A B C

Figure 2. (A) Transverse image of OSA at the level of the mid tibia. There is patchy hyperattenuation within the medullary cavity of the affected limb which is absent in the contralateral limb (B) at the same level. (C) A histologic slide made at the level of (A) shows evidence of mesenchymal neoplasia with osteoid production, consistent with OSA.

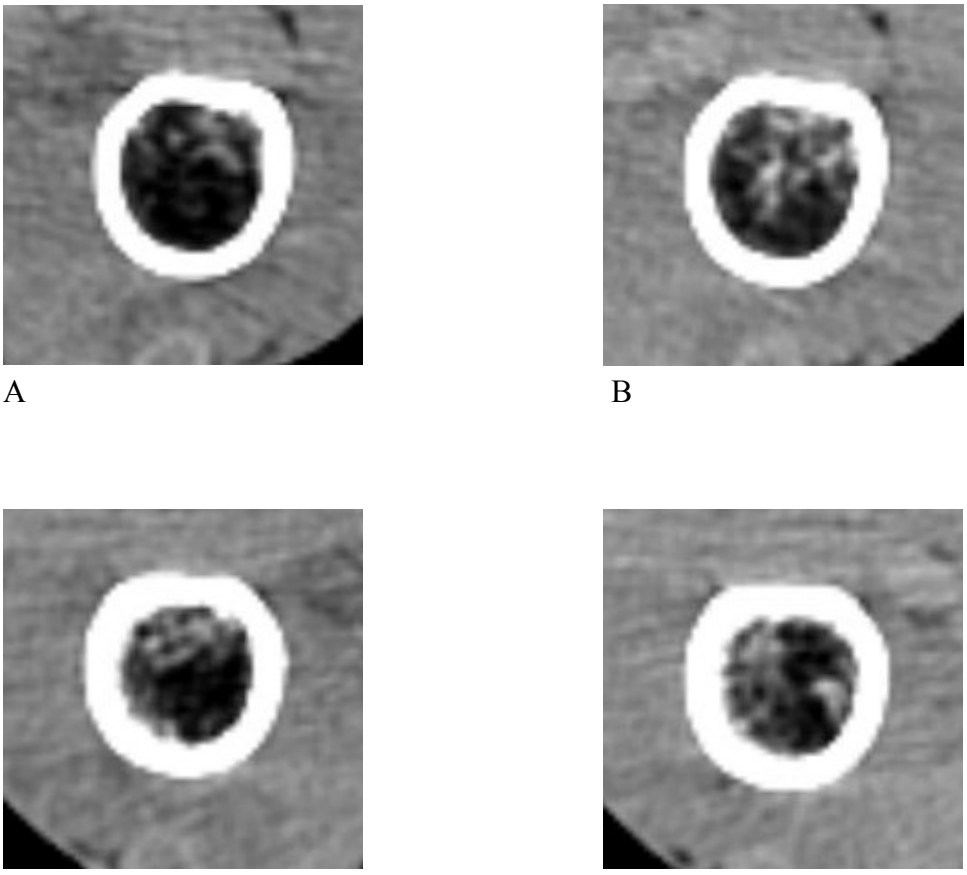

A B

C D

Figure 3. Abnormal contrast enhancement of distal femoral OSA. Transverse image of the affected limb pre-contrast (A) and post contrast (B) and the contralateral limb at the same level pre-contrast (C) and post contrast (D). There is an intramedullary increase of 53.6 HU post contrast in the affected limb using circular regions of interest compared to 5.2 HU in the contralateral limb, suggesting abnormal contrast enhancement of the limb with OSA (window width = 350, window level = 50).

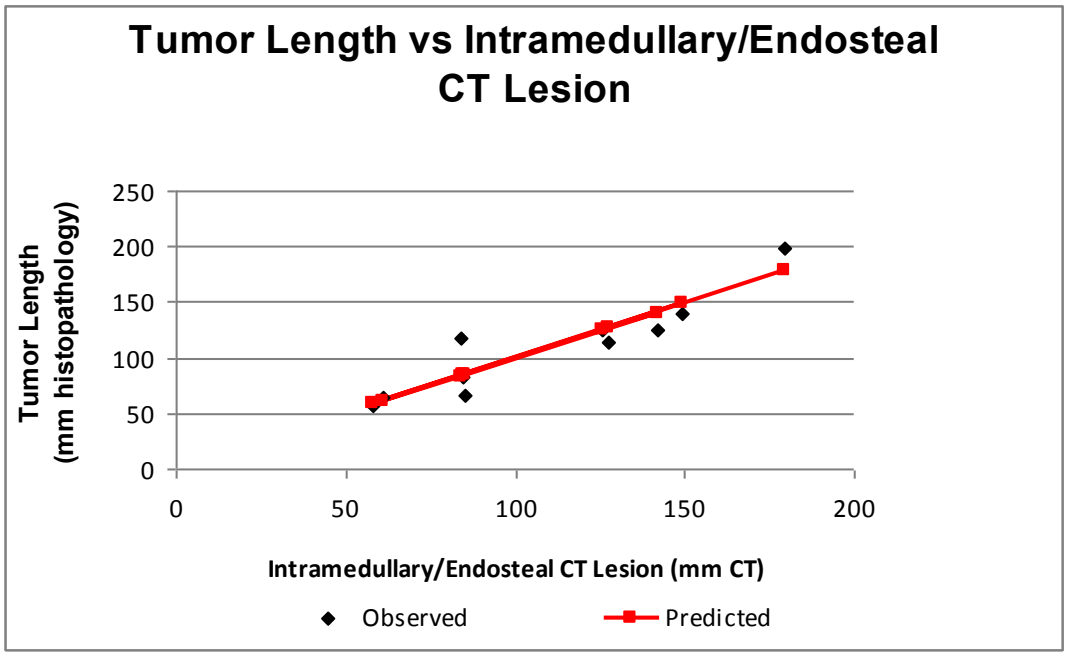

Figure 4. There is good correlation of tumor length based on histopathology compared to the length of intramedullary/endosteal abnormalities based on CT. There is good correlation of the data to the regression line ($r^2 = 0.85$). The slope of the regression line is 0.98 with a y-intercept of 1.1, indicating a near direct linear relationship. P-value = 0.0001.

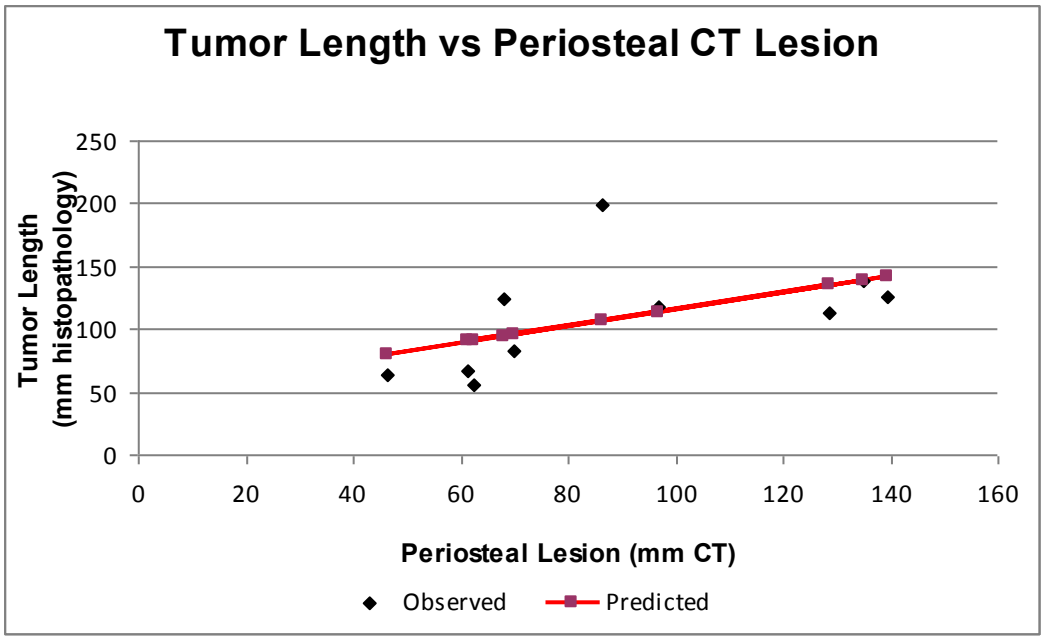

Figure 5. There is poor correlation of tumor length based on histopathology compared to the length of periosteal proliferation based on CT. Slope = 0.67, y-intercept = 49.4, r^2 = 0.27, p-value = 0.1225.

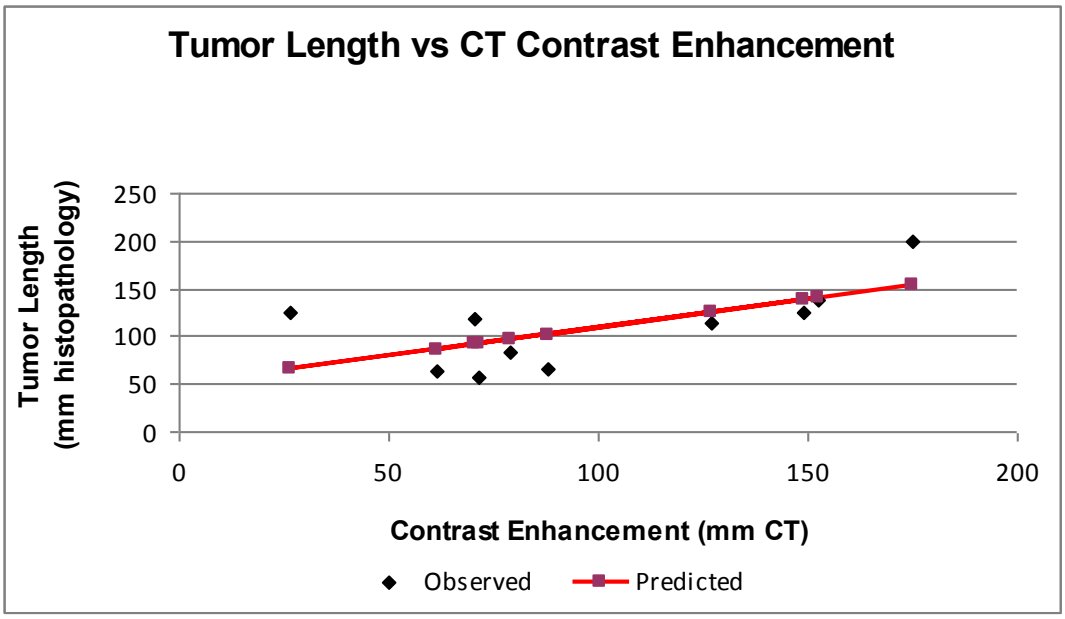

Figure 6. There is poor correlation of tumor length based on histopathology compared to the length of abnormal contrast enhancement based on CT. Slope = 0.59, y-intercept = 50.1, $r^2 = 0.42$, p-value = 0.0419.

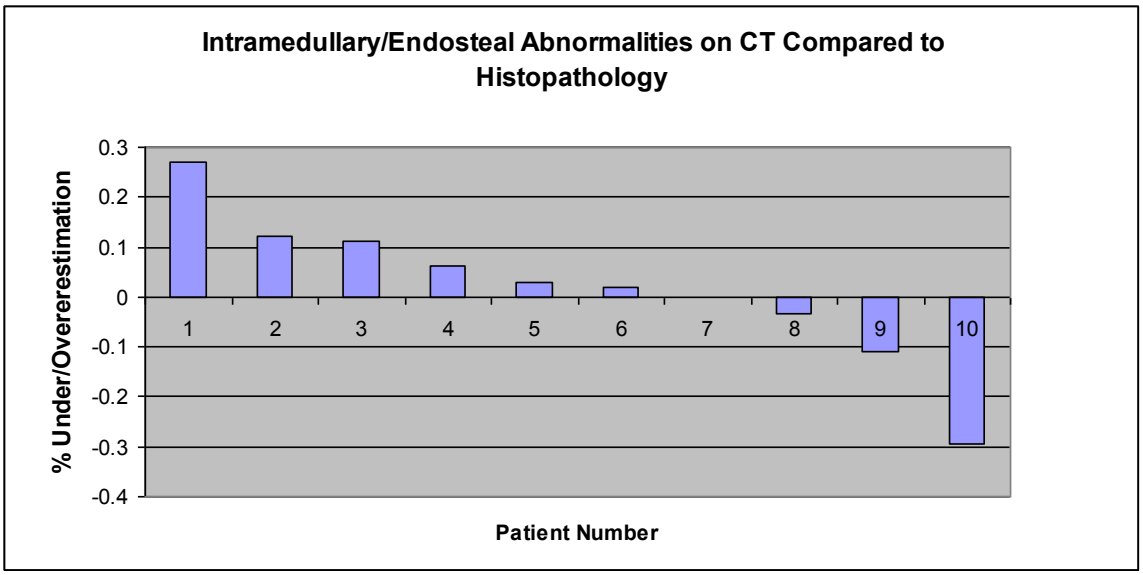

Figure 7. Distribution of percent overestimation and underestimation of the predictive value of intramedullary/endosteal abnormalities on CT compared to the true length of neoplasia based on histopathology.

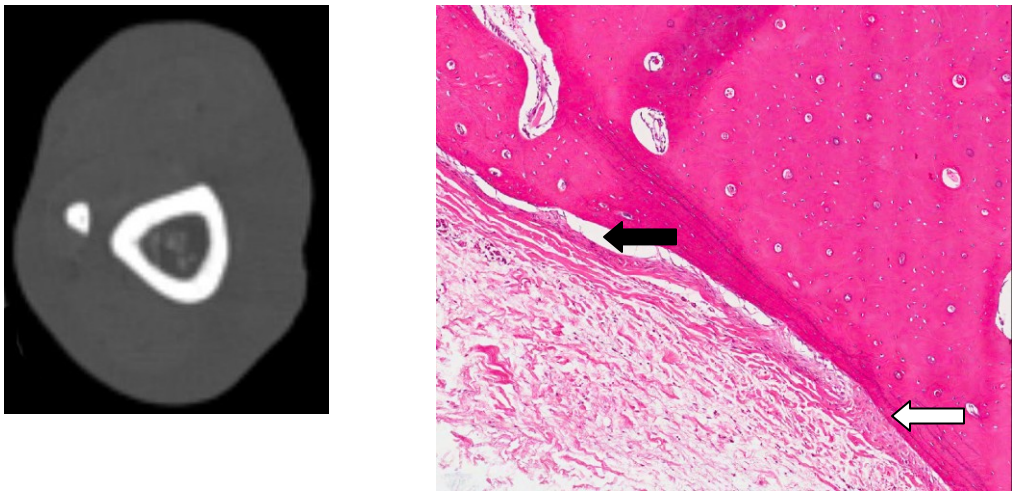

Figure 8. (A) Transverse CT image of OSA of the tibia. Note the lack of periosteal proliferation. (B) Histopathologic slide at the same level. There is evidence of periosteal hyperplasia (black arrow) transitioning from a more normal periosteum (white arrow).